Hindawi
Mathematical Problems in Engineering
Volume 2022, Article ID 6375727, 10 pages
https://doi.org/10.1155/2022/6375727

Research Article

A Multi-DOF Manipulator Joint Trajectory Tracking and Monitoring Method Based on Decision Tree

Qiong Wu,[1] **Hua Chen**,[2] **and Baolong Liu**[1]

[1]*Xi'an Technological University, School of Computer Science and Engineering, Xi'an 710021, China*
[2]*Xi'an Technological University, College of Mechanical and Electrical Engineering, Xi'an 710021, China*

Correspondence should be addressed to Hua Chen; chenhua@mjcedu.cn

Received 24 May 2022; Revised 30 August 2022; Accepted 7 September 2022; Published 15 October 2022

Academic Editor: Parikshit Narendra Mahalle

Understanding trajectory tracking control concerns is crucial for industrial-grade manipulators to provide precise and risk-free operations for the safe environment. Consequently, the robot arms need precise aim for tracking a given target trajectory by the trajectory control input driving torque which can use smart AI-based techniques for precision. Similarly, a decision tree is a soft computing-based method of feature space partitioning which can certainly allow the movement of robots in an accurate manner. The control of robot arms is an important aspect for automating the process of sustainable development. Aiming at the problem of poor tracking accuracy of traditional Multi-Degree-of-Freedom Manipulator Joint Trajectory Monitoring (Multi-DoF MJTM) and long monitoring delay, this article proposes a Multi-DOF manipulator joint trajectory tracking method based on decision tree. The Multi-DoF manipulator is developed for the adaptive control object of the working machine, and it is combined with the output response feature to construct the kinematics model of the Multi-DoF manipulator mechanism of the walking machine. The joint trajectory reconstruction of the running trajectory is used to obtain the joint trajectory deviation of the Multi-DoF manipulator's running trajectory through the multi-measurement system. Based on this, the Multi-DoF manipulator's running trajectory joint trajectory tracking control equation is obtained to realize the joint trajectory tracking and monitoring of the manipulator. The features for a safe environment are also integrated. The experimental results show that the proposed method has high accuracy in tracking the trajectory of Multi-DoF manipulator joints, and the time delay for tracking and monitoring the trajectory of manipulator's joints is also optimized.

1. Introduction

In recent years, robotic arm technology has developed rapidly, combined with multidisciplinary theories such as automatic control theory, mechanical engineering, electronic technology, and artificial intelligence, and its application range has also expanded from the industrial manufacturing field to medical, military, aerospace, and other precision industries. Robots are widely utilized in the building and infrastructure industries. Given the importance of human lives in both the development process and the environments in which robots operate, they must be precise. The accuracy of robots is important in sustainable development. Multi-DoF manipulator technology has been continuously developed and has become indispensable core automation equipment in the traditional manufacturing field. Its development is inseparable from the needs and development of industrial automation. The industrial manipulator is not simply a replacement for manual labor, but an intelligent mechanical device that integrates human and machine expertise [1]. It replaces people in industrial production to do certain repetitive, monotonous, long-term tasks, or high-risk operations in harsh environments. With the rapid development of modern industry, a higher-quality robotic arm is needed to serve it, and the working speed and precision requirements of the robotic arm are getting higher and higher. All this has prompted scholars from various countries to apply modern control theory to the robotic arm control system to solve the control problem of the robotic arm more efficiently [2].

Two approaches to resolving the singularity were presented in the literature [3], and both approaches may take place when the manipulator travels along a certain trajectory. A local genetic algorithm underlies one approach, while a global genetic algorithm underpins the other. Each approach's performance is evaluated using polynomial trajectories of up to three layers by assessing trajectory inaccuracy, the number of singular points, and the computing cost. The data show that the approach based on the global genetic algorithm works best when it follows the third-order trajectory since it has the lowest error, singularity, and computing cost. In [4], authors present a decision tree-based technique for investigating the issue of regulating the joint trajectories of Multi-DOF manipulators. The trajectory tracking control of the manipulator's end is performed using a proportional-integral-derivative (PID) sliding mode controller based on the manipulator's sliding mode surface. The sliding mode control simulation results are compared to the recommended sliding mode control simulation results. The literature [5] proposed the trajectory size to control the trajectory during the tracking process of the manipulator. In a three-dimensional, fully immersive virtual reality setting, a series of trajectories of varying lengths is planned out, and the object is given instructions for controlling the robotic arm so that it can track a cube target as it moves along the planned path. With a high-resolution motion capture system constantly monitoring the user's hand, the robotic arm may be moved to whatever location the user specifies. They compute the root mean square error, standard deviation of velocity, amplitude of acceleration rate, integral of velocity power spectrum, and 3D fuzzy approximation entropy to characterize the kinematics of a system. All kinematics markers rise considerably as the trajectory size increases, with the exception of IVPS between one-dimensional and two-dimensional circumstances and fApEn 3D between two-dimensional and three-dimensional situations. In higher dimensions, increasing time-domain parameters results in a loss in accuracy, energy efficiency, and multi-joint coordination. Under high-dimensional situations, the rise in frequency domain measurement represents the intermittent increase in visual feedback connected to human control when the trajectory size is increased. Larger nonlinear 3D values in 2D and 3D circumstances may be created by greater neuromotor noise and sensory input. The characteristics selected may give a complete method for measuring motor function from several viewpoints. In [6], author proposes an obstacle avoidance algorithm to solve the final trajectory planning issue for the duplicate manipulator, with the final trajectory's accuracy guaranteed to be within the predicted error. This is done by replacing the standard Euclidean distance with the vector pseudo distance to describe the closest possible distance between the robot arm and the obstacle. Five degrees-of-freedom (DOF) robot manipulators' positions may now be precisely controlled thanks to the author's research into and development of a new robust control [7]. Determining a Multi-DOF robot manipulator's precise mathematical model is a time-consuming task [7]. The above methods all have certain applicability in the tracking and monitoring of Multi-DoF manipulator joint trajectory, but the accuracy of tracking the manipulator joint trajectory still needs to be improved.

To solve the above problems, this paper proposes a Multi-DoF MJTM method based on decision tree. Kinematics analysis of the Multi-DoF manipulator is performed, and the adaptive follow-up control object and output response characteristic quantity are developed to build the Multi-DoF manipulator mechanism of the walking machine. In Kinematics model; the decision tree algorithm is introduced to discretize the joint trajectory data of the manipulator, and the deviation of the joint trajectory of the Multi-DoF manipulator is measured through the multi-measurement system, and the degree of deviation of the operation is obtained. On this basis, the decision tree algorithm reconstructs the joint trajectory of the manipulator's trajectory, and obtains the Multi-DoF manipulator trajectory joint trajectory tracking control equation through the degree of deviation of the manipulator's shutdown trajectory to realize the joint trajectory tracking and monitoring of the manipulator.

1.1. Major Highlight of the Paper

(1) Paper discuses about walker's Multi-DoF manipulator force adaptively follows the control object.

(2) Equation based on dynamic model of Multi-DoF manipulator of walking machine.

(3) How tracking and monitoring manipulator joint trajectory based on decision tree algorithm work.

(4) Measurement of the deviation of the joint trajectory of the robot arm.

(5) Reconstruction of joint trajectory.

(6) The suggested approach is tested experimentally, and the results are compared to those found in [3, 5].

This paper is structure as follows: Section 2 discuss in detail about kinematics analysis of Multi-DoF manipulator. In section 3 tracking and monitoring manipulator joint trajectory based on decision tree algorithm is proposed. Section 4 analysis proposed method based on some experiment. Section 5 finally concludes the study.

2. Kinematics Analysis of Multi-DoF Manipulator

The kinematics of a Multi-DoF manipulator mainly studies the relationship between the joint variables of the manipulator and the pose of the end effector. It can be used to complete the derivation of the dynamics model of the manipulator, trajectory planning, and the realization of trajectory tracking control. The establishment process of the equation and analyze its operating state and force. Furthermore, the kinematics equations and dynamics models of the manipulator are established to provide a solid theoretical foundation for the follow-up research on the tracking and monitoring of the manipulator's joint trajectory.

A Multi-DoF manipulator is formed by a series of links connected by joints. Therefore, a geometric relationship that describes the movement of the end of the link relative to a fixed reference coordinate system is required. This geometric relationship is a matrix method that combines the links in three-dimensional space. The position and posture of the subject are expressed as an equivalent homogeneous transformation matrix form, and then a link coordinate system is established on each link of the robot arm, and the geometric parameters of the complex robot arm are expressed in the coordinate system, and these parameters are used to describe the relationship between each link coordinate system.

2.1. Walker's Multi-DoF Manipulator Force Adaptively Follows the Control Object. In order to realize the adaptive follow-up control of the Multi-DoFmanipulator force of the walking machine, it is first necessary to construct the controlled object model of the Multi-DoF manipulator force adjustment of the walking machine, and adopt the underactuated mechanism power method for the Multi-DoF manipulator force adaptive following adjustment, mechanical adaptive follow-up control is carried out with two sets of force adjustment models of plane and lateral motion [8, 9], and the dynamic model of the Multi-DoF manipulator of the walking machine is described by the differential equations as follows:.

$$\begin{cases} mV = -mg\ \sin\dot{\theta} - c_x q S_M + P, \\ mV\dot{\theta} = -mg\ \cos\ \theta + c_y^{\alpha} q S_M \alpha + p\left(\alpha + \delta_{\varphi}\right) + m_R l_R \ddot{\delta}_{\varphi}. \end{cases} \tag{1}$$

Among them, the variables describing the longitudinal motion of the Multi-DoF manipulator arm adaptively follow the strength of the walking machine are $\varphi, \dot{\phi}, \alpha, \theta, \delta_{\varphi}$, etc., c is the movement distance of the Multi-DoF manipulator arm of the walking machine, and q is the motion of the multi-degree freedom manipulator arm of the walking machine. Speed, S_M is the amount of motion stability. $m_R l_R$ are the mass and length of the Multi-DoF manipulator arm of the walking machine. The plane underdriving mechanism is reduced in order, and the input state variable of force adaptive follow is selected as as $x = [\varphi, \dot{\varphi}, \theta]^T$ to construct a fitting relationship. The underdriving correction method of the flexible moving pair is used to correct the force measurement error of the Multi-DoF manipulator of the walking machine. The mechanical measurement equation of the Multi-DoF manipulator arm of the walking machine with the vertical x-axis in the positive direction of the y-axis is expressed as $\dot{x} = f(x, u)$. Under the condition that the control input variables of the Multi-DoF manipulator arm of the walking machine are determined, the mixed transmission of the flexible multi-body system is obtained. The driving force output state quantity $x_0 = [\varphi_0, \dot{\varphi}_0, \theta_0]^T$, according to the feedback correction of the measurement error, fully considering the effects of underdriving and flexibility, and obtaining the output balance condition: $f(x_0, u_0) = 0$. The state quantity of the longitudinal motion of the Multi-DoF manipulator operation of the walking machine is $x = [\varphi_0 + \Delta\varphi, \dot{\varphi}_0 + \Delta\dot{\varphi}, \theta_0 + \Delta\theta]^T$, $\delta_{\varphi} = \Delta\delta_{\varphi}$. Therefore, the mechanical control equation of the Multi-DoF manipulator arm of the walking machine is given by the following equation:

$$\begin{aligned} mV\Delta\dot{\theta} = &\left(c_y^{\alpha} q S_M + P\right)\Delta\alpha + mg\ \sin\ \theta\Delta\theta + P\Delta\delta_{\varphi} \\ &+ m_R l_R \Delta\ddot{\delta}_{\varphi}. \end{aligned} \tag{2}$$

According to the abovementioned analysis of the dynamic model of the Multi-DoF manipulator arm of the walking machine [10], the controlled object model of the original moving parts of each component of the Multi-DoF manipulator arm of the walking machine is described as the following equation:

$$\begin{cases} \Delta\dot{\theta} = c_1\Delta\alpha + c_2\Delta\theta + c_3\Delta\delta_{\phi} + c_3''\Delta\ddot{\delta}_{\varphi} + \overline{F}_{gr}, \\ \Delta\dot{\varphi} = b_1\Delta\dot{\phi} + b_2\Delta\alpha + b_3\Delta\delta_{\phi} + b_3''\Delta\ddot{\delta}_{\varphi} + \overline{M}_{gr}, \\ \Delta\varphi = \Delta\theta + \Delta\alpha. \end{cases} \tag{3}$$

Among them, $c_1 = 1/mV\,(57.3qS + P)$, $c_2 = 1/Vg\ \sin\ \theta$, $c_3 = P/mV$, $b_1 = 57.3/J_{z1}VSl_k^2$, and $b_2 = 57.3/J_{z1}qS\,(x_g - x_T)$, respectively, represent the known coefficients of the model and the control parameter input of the Multi-DoF manipulator of the walking machine in each radial channel, and the subscript k is the value of k operations.

2.2. Dynamic Model of Multi-DoF Manipulator of Walking Machine. Analyze the output response characteristic quantity of the strength of the Multi-DoF manipulator of the walking machine under abrupt conditions, and analyze the kinematics and dynamics model of the Multi-DoF manipulator mechanism of the walking machine [11]. Under the given parameters, set the step. The learning step length of the force control of the Multi-DoF manipulator arm is η. After n steps of training, the kinematics iterative equation of the Multi-DoF manipulator arm is obtained as the following equation:

$$W(n+1) = W(n) - \eta\frac{\partial E}{\partial W} + \partial\Delta\ W(n). \tag{4}$$

Among them, W is to select the appropriate stiffness and the driving torque of the original moving part, E is the moment of inertia, the output is $x_1, x_2, \ldots, x_n$ and the weight value 4 $w_{1j}, w_{2j}, \ldots, w_{nj}$ are, respectively, multiplied by the weight value, and the Multi-DoF machine of the walking machine is obtained. The arm strength adaptive following adjustment function is obtained by the following equation:

$$\begin{aligned} \frac{\partial E}{\partial w_j'} &= \frac{\partial E}{\partial v}\cdot\frac{\partial v}{\partial w_j'} \\ &= -\frac{2}{m}\sum_{k=1}^{m}[r(k) - y(k)]\frac{\partial y}{\partial v}x_j'(k). \end{aligned} \tag{5}$$

Deriving the speed equation of the mechanism, the kinematics model of the Multi-DoF manipulator mechanism of the walking machine is obtained by the following equation:

$$\frac{\partial E}{\partial w_{ij}} = \frac{\partial E}{\partial v}\frac{\partial v}{\partial x''}\frac{\partial x''}{\partial u''}\frac{\partial u''}{\partial I''}\frac{\partial I''}{\partial x_j'}\frac{\partial x_j'}{\partial u_j'}\frac{\partial u'}{\partial I_j'}\frac{\partial I_j'}{\partial w_{ij}}$$

$$= -\frac{1}{m}\sum_{k=1}^{m}\delta'(k)w_j'\mathrm{sgn}\frac{u_j'(k)-u_j'(k-1)}{I_j'(k)-I_j'(k-1)}x_i(k) \quad (6)$$

$$= -\frac{1}{m}\sum_{k=1}^{m}\delta_j(k)x_i(k).$$

Through nonlinear strict feedback, the kinematics model of Multi-DoF manipulator force adaptive follow-up of the walking machine is constructed [12], and the dynamic model of the mechanism established by Lagrangian method is given by the following equation:

$$w'(n_0+1) = w'(n_0) - \eta'\frac{\partial J}{\partial w'}. \quad (7)$$

The error compensation of the force adaptive follow-up control is accomplished by the analysis of the dynamic model of the Multi-DoF manipulator of the walking machine, and the adaptive adjustment capacity of the multi-degree-of-freedom manipulator of the walking machine is optimized.

3. Tracking and Monitoring Manipulator Joint Trajectory Based on Decision Tree Algorithm

3.1. Decision Tree Algorithm. The use of the decision tree algorithm is generally divided into two steps. First, train the existing data to obtain the model of the decision tree, and then classify the unclassified data according to the obtained decision tree model. Decision tree is a tree shape, its nodes are divided into leaf nodes and branch nodes [21, 22]. The primary and secondary order is from top to bottom, from left to right.

At first, it was just an empty tree and a collection of processed data samples. When performing data allocation, select the optimal root node, and also select the attributes of the test, and then divide the data in the sample. The decision tree generation process the following points:

(1) If the attributes in the current sample set belong to the same category, then only the leaf nodes of this category are created

(2) If it is not the same attribute, select the optimal calculation method to calculate any possible division method of the current set

(3) Consider the node's attribute to be the one corresponding to the ideal partition, then make as many child nodes as the attribute

(4) For each node, a sample set is partitioned into child nodes based on the value of an attribute chosen to represent the node's condition

(5) Regard the branched node as the current node, and then repeat from step (2), and guide the final division until it is complete, as shown in Figure 1

Scholars have always been committed to the study of more effective decision tree algorithms, and successively developed ID3 algorithm and C4.5 algorithm to get the best decision tree. The following is a brief introduction to common ID3 decision trees. ID3 algorithm is a classic algorithm in decision tree algorithms. It uses information gain as the basis for attribute selection, then classifies the training set of samples, and uses entropy in information theory to calculate information gain including information entropy and information conditional entropy. Information entropy can measure the degree of ordering of the data set in the system. The larger the information entropy, the more chaotic the information in the system, and the smaller the entropy, the more orderly in the system. It can be expressed as the following equation:

$$I(C) = -\sum_{i=1}^{m}P(C_i)\log_2 P(C_i). \quad (8)$$

In the formula, $P(C_i)$ is the probability of C_i in the m category. The expression method of conditional entropy of attribute A is given by the following equation:

$$E(A) = -\sum_{j=1}^{n}P(A_i)\sum_{j=1}^{m}P(C_i|A_i)\log_2 P(C_i|A_i). \quad (9)$$

According to the obtained information entropy and conditional entropy, the gain of attribute A can be calculated. It can be seen that in order to obtain the gain of information through the ID3 algorithm, the premise is that the attributes of the sample concentration are discrete. If there is a continuous one, it should be discretize in advance.

3.2. Measurement of the Deviation of the Joint Trajectory of the Robot Arm. Three measuring systems are used to measure the degree of deviation of the joint trajectory of the Multi-DoF manipulator. Figure 2 shows the angle of the orientation of the Multi-DoF robotic arm measurement system.

Analyze the working principle of the measurement system in combination with Figure 2. Define X to measure the angle between the host and the x axis, Y to measure the angle between the slave 1 and the y axis, and Z to measure the angle between the slave 2 and the z axis. The angle conversion method is as given by the following equations:

$$X = r\cos b\cos a, \quad (10)$$

$$Y = r\cos b\sin a, \quad (11)$$

$$Z = r\cos b + \frac{1-k}{2A}r^2. \quad (12)$$

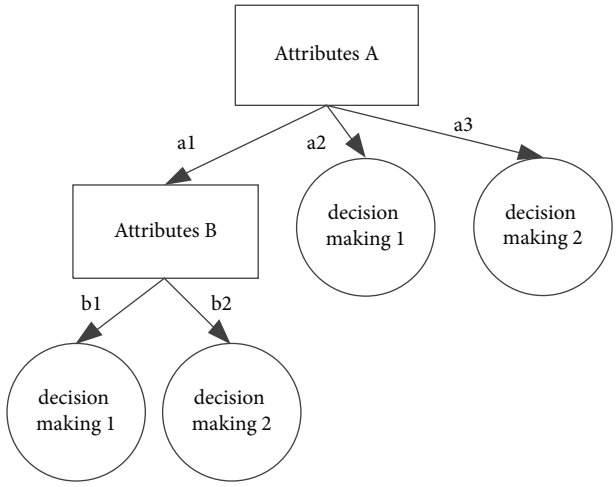

Figure 1: Decision tree algorithm.

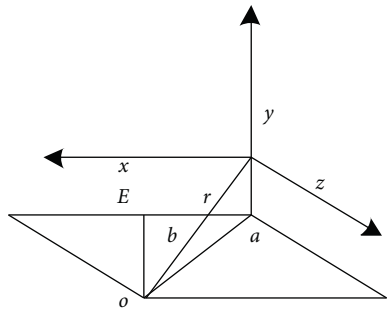

Figure 2: The angle formed by the displacement measurement position of the multi-degree-of-freedom manipulator.

In the formula: a, b are the measurement horizontal angle and vertical angle, respectively; r is the master slope distance; k is the measurement error coefficient of the slave machine; and A is the master horizontal distance.

Define the coordinate component accuracy of the master and slave points (x, y, and z) of the measurement system based on the law of error inertia. The indicators are as given in the following equations:

$$e^2X = \left(\frac{X\varphi}{\partial}\right)^2 e^2\partial + X^2\varphi[\tan\ a + \cot(a+b)]^2 \times \left(\frac{e}{\varphi}\right)^2 + X^2\varphi[\cot\ b - \cot(a+b)]^2 \times \left(\frac{e}{\varphi}\right)^2, \tag{13}$$

$$e^2Y = \left(\frac{Y\varphi}{\partial}\right)^2 e^2\partial + Y^2\varphi[\tan\ a + \cot(a+b)]^2 \times \left(\frac{e}{\varphi}\right)^2 + Y^2\varphi[\cot\ b - \cot(a+b)]^2 \times \left(\frac{e}{\varphi}\right)^2, \tag{14}$$

$$\begin{aligned} e^2Z = {} & \left[\frac{Z - l/2}{\partial}\right]^2 e^2\partial + \left\{Z^2\cot^2(a+b) + (Z-l)^2\left[\cot\ a - \cot\ (a+b)^2\right]\right\}\left(\frac{e}{\varphi}\right)^2 \\ & + \left\{Z^2\left[\cot\ b - \cot(a+b) + (Z-l)^2\cot^2(a+b)\right]\right\} \\ & \cdot \left(\frac{e}{\varphi}\right)^2 + \left[\frac{Z}{\sin(2\theta)}\right]^2\left[\frac{e}{\varphi}\right]^2 + \left[\frac{Z-l}{\sin(2\theta)}\right]^2\left(\frac{e}{\varphi}\right) + \frac{1}{4}e^2l. \end{aligned} \tag{15}$$

In the formula, ∂ is the deviation coefficient measured by the host computer; φ, e, l, respectively, are the arm section variable difference, error inertia coefficient, and error value of the manipulator; θ is the deviation angle.

Based on the above steps, the multi-machine joint measurement system is used to complete the measurement of the joint trajectory deviation of the manipulator's operating trajectory. According to the result, the joint trajectory of the operating trajectory can be

automatically controlled to ensure that the manipulator is running back on track.

3.3. Tracking and Monitoring Method of Robotic Arm Joint Trajectory

3.3.1. Reconstruction of Joint Trajectory. On the premise of parameter modification, the trajectory reconstruction of the manipulator is completed by the method of reconstruction of the motion space of seven-degrees-of-freedom. Fuzzy approach used in [13] is used in the research. Assuming that the manipulator control input parameters have single-point fuzzy characteristics because the manipulator is subject to linear disturbances, considering the degree of deviation of the manipulator's motion trajectory and joint trajectory, combined with the adjusted motion trajectory and joint trajectory parameters to construct the longitudinal motion parameter objective function and system dynamics transfer function [14, 15] as shown in equations (16) and (17), both functions include certain and uncertain parts:

$$\begin{aligned} B &= B_n + \Delta B, \\ h\left(\lambda_\alpha, \dot{\lambda}_\alpha\right) &= h_n\left(\lambda_\alpha, \dot{\lambda}_\alpha\right) + \left(\Delta h\left(\lambda_\alpha, \dot{\lambda}_\alpha\right) + X_\phi + Y_\phi + Z_\phi\right), \end{aligned} \tag{16}$$

where B is the nonlinear disturbance; B_{n} is the fuzzy membership determination of the manipulator; ΔB is the mean value of the fuzzy membership determination; $h(\lambda_\alpha, \dot{\lambda}_\alpha)$ is the nonlinear determination; $h_n(\lambda_\alpha, \dot{\lambda}_\alpha)$ is the linear uncertainty; $\Delta h(\lambda_\alpha, \dot{\lambda}_\alpha)$ is the linear coefficient; λ_α is the moving target position point; and $\dot{\lambda}_\alpha$ is the moving position point of the moving target [16, 17].

During the adjustment process, each parameter needs to satisfy the following formula:

$$B_n \ddot{\lambda}_\alpha + h_n\left(\lambda_\alpha, \dot{\lambda}_\alpha\right) = u(t) + \rho(t), \tag{17}$$

where $\ddot{\lambda}_\alpha$ is the function to increase the output; $\rho(t)$ is the end linear velocity of the manipulator; and $u(t)$ is the external torque, which is mainly used to optimize the control function.

On the basis of calculating the mechanical arm dynamic coefficient, unknown nonlinear function vector, and fuzzy rule characteristic value, the decision tree algorithm is used to describe the grasping state trajectory of the mechanical arm [18]. The adaptive online adjustment parameters can solve the problem of large disturbance. Let $\overline{\rho}(t)$ be the mechanical arm grasping take the uncertainty upper limit, which should meet the (18) following equation conditions:

$$|\rho(t)| < |\overline{\rho}(t)|. \tag{18}$$

Equation (19) describes the sliding surface of the joint trajectory control of the manipulator trajectory as follows:

$$B_n \ddot{\lambda}_\alpha - \beta_1 h_n\left(\lambda_\alpha, \dot{\lambda}_\alpha\right) = \overline{\rho}(t) + B_n f_d. \tag{19}$$

In the formula, β_1 is the expansion factor to be optimized; f_{d} is the joint trajectory parameter of the adaptive control running trajectory. On this premise, reconstruct the seven-degree-of-freedom motion space to obtain the trajectory of the robotic arm. The equation is given by

$$\beta_1 \ddot{\lambda}_\alpha + f_d = B_n \ddot{\lambda}_\alpha + h_n\left(\lambda_\alpha, \dot{\lambda}_\alpha\right). \tag{20}$$

3.3.2. Running Trajectory Joint Trajectory Tracking Monitoring Method. On the premise of reconstructing the joint trajectory of the manipulator trajectory, the optimal control law of the joint trajectory of the manipulator trajectory is calculated to complete the joint trajectory tracking and monitoring.

In addition to the joint trajectory deviation of the running trajectory measured by the multi-machine joint measurement system, external factors such as flexibility and friction will also cause certain interference to the joint trajectory of the manipulator's running trajectory [19]. This interference error can be expressed a given equation (2).

$$\begin{cases} q_1 = \lambda_\alpha - \dot{\lambda}_\alpha, \\ q_2 = \ddot{\lambda}_\alpha - \dot{\lambda}_\alpha. \end{cases} \tag{21}$$

In the formula, q_1, q_2, respectively, flexible error and rigid error.

The kinematic errors caused by the bearing and transmission mechanism can cause the attitude angle of the manipulator to change. The torque deviation error N_1, N_2 caused by the flexibility error and the rigid error can be expressed as equation

$$\begin{cases} N_1 = \ddot{\lambda}_\alpha q_1, \\ N_2 = B_n^{-1} q_2 - B_n^{-1} h_n\left(\lambda_\alpha - \dot{\lambda}_\alpha\right) - \ddot{\lambda}_\alpha. \end{cases} \tag{22}$$

The above deviation error is optimized by the variable structure fuzzy control method, and the variable structure neural network model is constructed as equation.

$$\mathrm{net}_j = \sum_{i=1}^{n} \omega_{ij} x_i(t), \quad i \neq j, \tag{23}$$

where, net_j is the rate of change of synovial motion trajectory; $x_1, x_2, \ldots, x_n$ is the dynamic parameter of the joint trajectory of the manipulator's output trajectory; and $\omega_{1j}, \omega_{2j}, \ldots, \omega_{nj}$ is the weight value.

On the premise of the steady motion analysis result of the manipulator operating attitude angle control, the form of the sliding surface after error optimization is obtained as equation

$$v = \mathrm{net}_j\left(\mu q_1 + q_2\right), \tag{24}$$

where v is the optimized sliding mode surface; μ is the sliding mode coefficient.

The local elastic coefficient reflects the flexibility characteristics of the rear transmission device of the robotic arm joint

$$\dot{v} = \mathrm{net}_j(\mu N_1 + N_2). \tag{25}$$

Based on external dynamic constraints, calculate the mechanical arm longitudinal running transmission stiffness parameter $\mu v + \dot{v}$ as

$$\mu v + \dot{v} = \mu N_2 + \ddot{\lambda}_\alpha - \ddot{\lambda}_\alpha = \mu q_2 + B_n^{-1} - B_n^{-1} h_n\left(\lambda_\alpha, \ddot{\lambda}_\alpha\right) - \ddot{\lambda}_\alpha. \tag{26}$$

The construction of the optimal control law for manipulator operation is based on the premise that Taylor expands and obtains the torsion deformation of the manipulator transmission mechanism. The control law is described as

$$u_{qc} = h_n\left(\lambda_\alpha, \ddot{\lambda}_\alpha\right) + B_n \ddot{\lambda}_\alpha - B_n \mu \dot{v}, \tag{27}$$

where u_{qc} is the optimal control law of the robotic arm. When the variable structure fuzzy PID control algorithm is used to adjust the trajectory error, the predicted value of the manipulator joint torque u_0 is as the following equation.

$$u_0 = -\mathrm{sgn}(B_n)\overline{\rho}(t) + \mathrm{sgn}\left(u_{qc}\right). \tag{28}$$

According to (28), the dynamic control equation for the deviation of the joint trajectory of the Multi-DoF manipulator can be output as

$$F\left(\lambda_\alpha, \dot{\lambda}_\alpha\right) = h_n\left(\lambda_\alpha, \dot{\lambda}_\alpha\right) + B_n \dot{\lambda}_\alpha - B_n \mu q_2 - u_0. \tag{29}$$

The above analysis process is combined to obtain the deviation value of the joint trajectory of the Multi-DoF manipulator, and the automatic control of the tracking and monitoring deviation of the Multi-DoF manipulator's trajectory can be completed.

4. Experimental Analysis

At present, the dynamic simulation of the manipulator system mainly uses MATLAB software simulation and co-simulation with Adams software. MATLAB has very good numerical and graphic processing functions. Adams is a professional mechanical system dynamics analysis software, based on the establishment of dynamic models, and can be seamlessly combined with MATLAB, so the use of co-simulation has obvious advantages. The software versions used in this paper are Adams 2013 and MATLAB 2010. The six-degree-of-freedom manipulator [20, 21] is used as the simulation experiment object, and the literature [3] method and the literature [5] method are used as the experimental comparison method to study the Multi-DoF based on the decision tree designed in this paper. The effectiveness of the monitoring method for tracking the trajectory of the robotic arm joints is verified.

4.1. Simulation of Six-Degree-of-Freedom Manipulator System. It is proposed that the end link of the six-degree-of-freedom manipulator maintains a fixed posture relative to the base coordinate system, so that the end points complete a set of smooth curve trajectories. The projection of the trajectory in the YZ plane is a circle with (0.34, −0.3) as the center and a radius equal to 0.1 m. The projection on the X axis changes according to the sine law, which can be expressed as the following equation:

$$\begin{cases} x = 0.01\ \sin(4t), \\ y = 0.34 - 0.1\ \cos(2t), \\ z = -0.3 - 0.1\ \cos(2t), \\ \psi = 0, \\ \theta = \dfrac{\pi}{2}, \\ \phi = 0. \end{cases} \tag{30}$$

First, set the simulation parameters, the simulation time is 30 s, the Runge-Kutta algorithm is used, and the fixed step is 0.01 s. Shown in Figures 3(a)–3(f) are the change curves of the angle of each joint of the six-degree-of-freedom manipulator system within 30 s. It can be seen from the simulation result graph that each curve is relatively smooth, there is no sudden change, and it is periodic.

4.2. Simulation Analysis and Result Processing. Under the construction of the above simulation model, the accuracy of tracking and monitoring the joint trajectory of the Multi-DoF manipulator designed in this paper is tested. The accuracy of trajectory tracking and monitoring is shown in Figure 4.

Analyzing Figure 4, it can be seen that the average tracking and monitoring accuracy of the robotic arm joint trajectory in the literature [3] method is 71%, and the average tracking and monitoring accuracy of the robotic arm joint trajectory monitoring in the literature [5] is 81%. The average tracking accuracy of arm joint trajectory monitoring is 94%. The method in this paper is more accurate in monitoring the trajectory of multi-free manipulator joints, and the monitoring effect is better.

On this basis, the time delay of three different methods for tracking and monitoring the robot arm joint trajectory is tested, and the comparison result is shown in Figure 5.

Analyzing Figure 5, it can be seen that the average tracking and monitoring delay of the robotic arm joint trajectory in the literature [3] method is 0.21 s, and the average tracking and monitoring delay of the robotic arm joint trajectory in the literature [5] method is 0.31 s. The average value of the trajectory tracking monitoring delay is 0.05 s. The shorter the monitoring delay, the better the real-time performance of this method. It can be seen that the method in this paper has better real-time performance for Multi-DoF MJTM and better monitoring effect it is good.

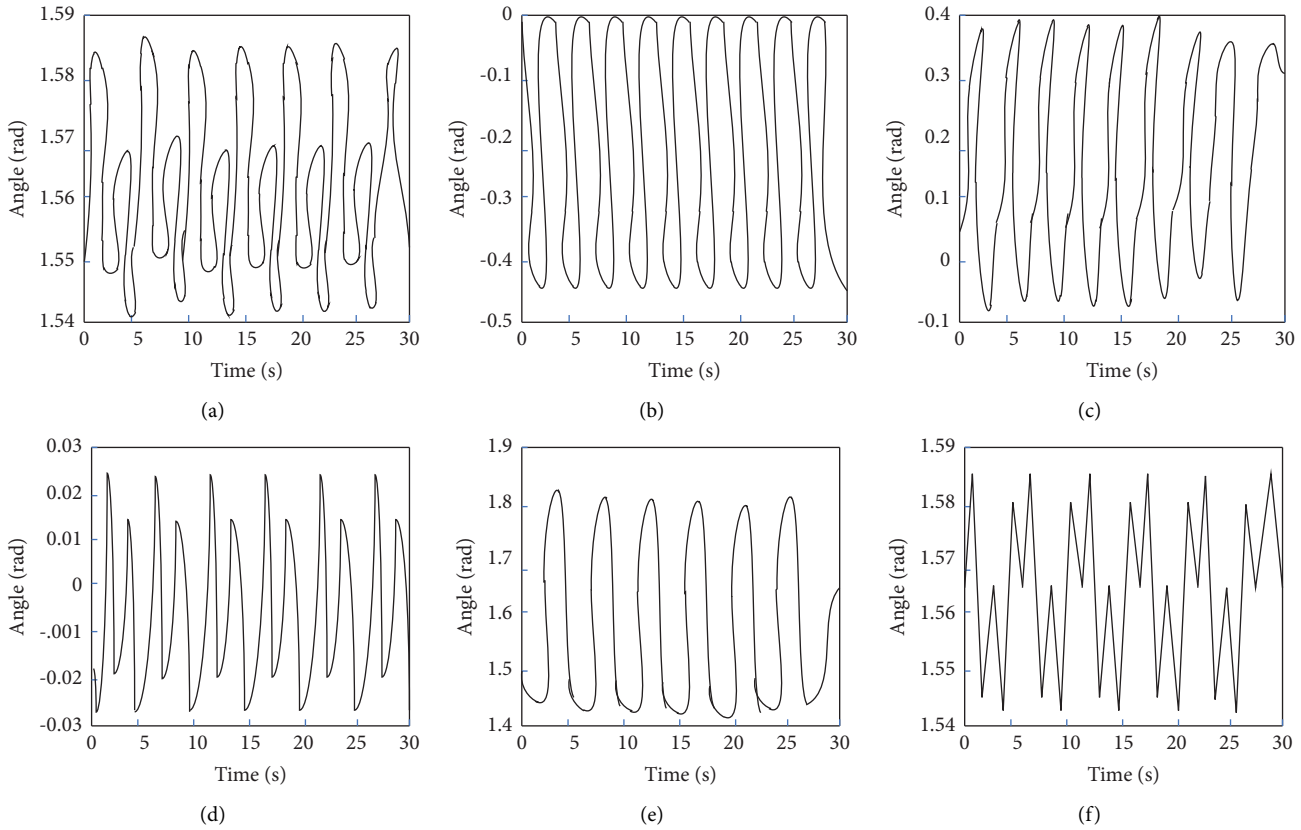

Figure 3: Robotic arm joint trajectory tracking control joint angle change curve. (a) Joint 1 angle curve. (b) Joint 2 angle curve. (c) Joint 3 angle curve. (d) Joint 4 angle curve. (e) Joint 5 angle curve. (f) Joint 6 angle curve.

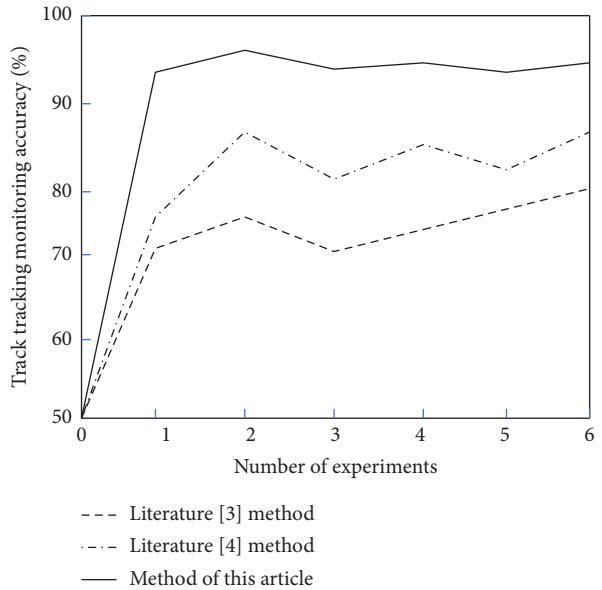

Figure 4: Comparison results of tracking and monitoring accuracy of robotic arm joint trajectory.

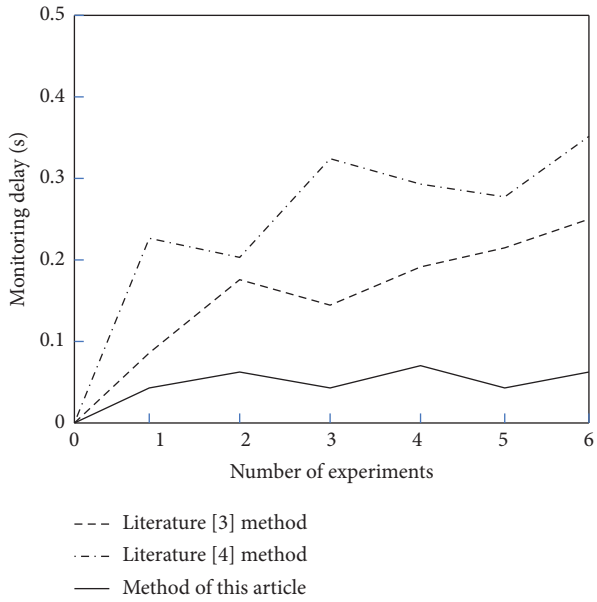

Figure 5: Comparison results of tracking and monitoring time delays of robotic arm joints.

5. Summary

As of now, there is a significant chasm between the theoretical discovery of industrial robotic machines and the practical application of robotic arm mechanics. Each nation must establish the fundamental technology for robotic weapons and actively encourage the development of sustainable industries in this field. This paper proposes a decision tree-based Multi-DoF manipulator joint trajectory tracking monitoring method. The kinematics analysis of the Multi-DoF manipulator, the adaptive follow-up control object of the Multi-DoF manipulator force of the walking machine, and the output response characteristic quantity are used to build the Multi-DoF manipulator mechanism of the walking machine. In the kinematics model; the decision tree method is used to discretize the manipulator's joint trajectory data. The deviation of the Multi-DoF manipulator's joint trajectory is monitored using a multi-measurement system to determine the operation's degree of deviation. In this paper, we compare the proposed method with two well-known existing methods, and the experimental results show that the designed method has high accuracy in tracking and monitoring the joint trajectory of the manipulator with a short time delay and has certain practical applicability. The future scope of this research is to increase the accuracy from 94% to above. This article also finds a way to improve the accuracy of the trajectory algorithm for 3D space.

Data Availability

All the data pertaining to this research are available in the article.

Conflicts of Interest

The authors declare that there are no conflicts of interest regarding the publication of this paper.

Acknowledgments

The research is supported by Natural Science Basic Research Program of Shaanxi Province (No. 2019JM-484) and Research on Intelligent Recommendation Method of Mobile Application Crowdsourcing Test Task based on deep reinforcement learning for the resources used in research work.

References

[1] TuanhuiS, W. Weibing, and J. Y. JinganF, "Research of Co-simulation of motion and control of manipulator clamping mechanism," *Computer Simulation*, vol. 36, no. 2, pp. 302–306, 2019.

[2] B. E. Demir, R. Bayir, and F. Duran, "Real-time trajectory tracking of an unmanned aerial vehicle using a self-tuning fuzzy proportional integral derivative controller," *International Journal of Micro Air Vehicles*, vol. 8, no. 4, pp. 252–268, 2016.

[3] P. P. Rebouças Filho, S. P. P da Silva, V. N. Praxedes, J. Hemanth, V. H. C. de Albuquerque, and C. Vhcda, "Control of singularity trajectory tracking for robotic manipulator by genetic algorithms," *Journal of Computational Science*, vol. 30, no. 2, pp. 55–64, 2019.

[4] G. Gao, C. Ou, and L. Shi, "Multi-Degree-of-Freedom manipulator joint trajectory tracking control method based on decision tree," *Journal of Physics: Conference Series*, vol. 2066, no. 1, Article ID 012026, 2021.

[5] M. Fan, J. Luo, L. Li, D. F. Huang, Y. Zhan, and R. Song, "Kinematic analysis of trajectory dimension-dependent sensorimotor control in arm tracking," *IEEE Access*, vol. 7, no. 1, pp. 8890–8900, 2019.

[6] H. Yang, D. Li, X. Xu, and H. Zhang, "An obstacle avoidance and trajectory tracking algorithm for redundant manipulator end," *IEEE Access*, vol. 10, pp. 52912–52921, 2022.

[7] S. J. Abbasi, H. Khan, and M. C. Lee, "Robust control design for the accurate trajectory tracking of multi degree of freedom robot manipulator," in *Proceedings of the 2021 18th International Conference on Ubiquitous Robots (UR)*, pp. 375–379, Gangneung, Korea (South), July 2021.

[8] P. Nancy, S. Muthurajkumar, S. Ganapathy, S. Santhosh Kumar, M. Selvi, and K. Arputharaj, "Intrusion detection using dynamic feature selection and fuzzy temporal decision tree classification for wireless sensor networks," *IET Communications*, vol. 14, no. 5, pp. 888–895, 2020.

[9] W. Tian, M. Lauer, and L. Chen, "Online multi-object tracking using joint domain information in traffic scenarios," *IEEE Transactions on Intelligent Transportation Systems*, vol. 21, no. 1, pp. 374–384, 2020.

[10] J. E. Lavín-Delgado, J. E. Solís-Pérez, J. F. Gómez-Aguilar, and R. F. Escobar-Jiménez, "Trajectory tracking control based on non-singular fractional derivatives for the PUMA 560 robot arm," *Multibody System Dynamics*, vol. 50, no. 3, pp. 259–303, 2020.

[11] H. Yan and Y. Han, "Decentralized adaptive multi-dimensional Taylor network tracking control for a class of large-scale stochastic nonlinear systems," *International Journal of*

Adaptive Control and Signal Processing, vol. 33, no. 4, pp. 664–683, 2019.

[12] X. W. Wang, J. Liu, Y. Zhang, B. Shi, D. Jiang, and H. Peng, "A unified symplectic pseudospectral method for motion planning and tracking control of 3D underactuated overhead cranes," *International Journal of Robust and Nonlinear Control*, vol. 29, no. 7, pp. 2236–2253, 2019.

[13] R. V. Patil, P. N. Mahalle, and G. R. Shinde, "Base for trust score estimation for device to device communication in internet of thing using fuzzy approach and machine learning," in *Security Issues and Privacy Threats in Smart Ubiquitous Computing. Studies in Systems, Decision and Control*, P. N. Mahalle, G. R. Shinde, N. Dey, and A. E. Hassanien, Eds., vol. 341, Singapore, Springer, 2021.

[14] B. Mareschal, M. Kaur, V. Kharat, and S. S Sakhare, "Convergence of smart technologies for digital transformation," *Tehnički glasnik*, vol. 15, p. 1, 2021.

[15] A. Kumar and A. K. Ghosh, "Decision tree- and random forest- based novel unsteady aerodynamics modeling using flight data," *Journal of Aircraft*, vol. 56, no. 1, pp. 403–409, 2019.

[16] E. Ezra and M. Sharir, "A nearly quadratic bound for point-location in hyperplane arrangements, in the linear decision tree model," *Discrete & Computational Geometry*, vol. 61, no. 4, pp. 735–755, 2019.

[17] P. R. Kadavi, C. W. Lee, and S. Lee, "Landslide-susceptibility mapping in Gangwon-do, South Korea, using logistic regression and decision tree models," *Environmental Earth Sciences*, vol. 78, no. 4, pp. 116–116.17, 2019.

[18] M. Kaur, S. Kadam, and N. Hannoon, "Multi-level parallel scheduling of dependent-tasks using graph-partitioning and hybrid approaches over edge-cloud," *Soft Computing*, vol. 26, no. 11, pp. 5347–5362, 2022.

[19] W. Fude, Z. Jigui, Y. Guifang, L. Pengfei, and H. Junrui, "Design and obstacle-climbing performance analysis of arm-wheeled robot based on creo and adams," in *Proceedings of the 2017 Chinese Automation Congress (CAC)*, pp. 7555–7559, Jinan, China, October 2017.

[20] C. Zhang and Y. Wu, "The motion planning of Six-Degree-of-Freedom manipulator based on P-Rob," in *Proceedings of the 2021 China Automation Congress (CAC)*, pp. 73–78, Beijing, China, October 2021.

[21] M. Yu, Y. Xu, S. Chen, and Y. Li, "Dynamic modeling and simulation of flexible joint manipulator," in *Proceedings of the 2021 IEEE 5th Advanced Information Technology, Electronic and Automation Control Confserence (IAEAC)*, pp. 259–263, Chongqing, China, March 2021.

[22] M. Kaur, A. Jadhav, and F. Akter, "Resource selection from edge-cloud for IIoT and blockchain-based applications in industry 4.0/5.0," *Security and Communication Networks*, Hindawi, vol. 2022, Article ID 9314052, 10 pages, 2022.